Lateral induced dipole moment and polarizability of excitons in a ZnO single quantum disk

F. Dujardin, E. Feddi, A. Oukerroum, J. Bosch Bailach, J. Martinez-Pastor, E. Assaid

Lateral induced dipole moment and polarizability of excitons in a ZnO single quantum disk

F. Dujardin, E. Feddi' , A. Oukerroum, J. Bosch Bailach, J. Martínez-Pastor, and E. Assaid

Citation: Journal of Applied Physics **113**, 064314 (2013); doi: 10.1063/1.4792047
View online: http://dx.doi.org/10.1063/1.4792047
View Table of Contents: http://aip.scitation.org/toc/jap/113/6
Published by the American Institute of Physics

Lateral induced dipole moment and polarizability of excitons in a ZnO single quantum disk

F. Dujardin,[1] E. Feddi,[2,a)] A. Oukerroum,[3] J. Bosch Bailach,[4] J. Martínez-Pastor,[4] and E. Assaid[5]

[1]*Laboratoire de Chimie et Physique des Milieux Complexes, Université de Lorraine, 1 Bd Arago, 57070 Metz, France*
[2]*ENSET de Rabat, Université Mohamed V Souissi, B.P. 6207, Rabat-Institut, Rabat, Morocco*
[3]*Laboratoire de Physique de la Matière Condensée, Faculté des Sciences et Techniques, B.P. 140, Bd Yassima, 28820 Mohammedia, Morocco*
[4]*Instituto de Ciencia de los Materiales, Universidad de Valencia, P.O. Box 2085, 46071 Valencia, Spain*
[5]*Laboratoire d'Electronique et Optique des Nanostructures de Semiconducteurs, Faculté des Sciences, B. P. 20, El Jadida, Morocco*

(Received 21 November 2012; accepted 29 January 2013; published online 14 February 2013)

The lateral Stark shift of an exciton confined in a single ZnO quantum thin disk of radius R was calculated using a variational approach within the two bands effective mass approximation. It is shown that the exciton has a non negligible induced dipole moment when an external electric field is applied mainly for electron-hole separation below to the 3D excitonic Bohr radius. The behavior of the exciton lateral Stark shift proves the existence of an important correlation between the polarizability and the induced dipole moment. © *2013 American Institute of Physics*. [http://dx.doi.org/10.1063/1.4792047]

I. INTRODUCTION

Nowadays, the zero dimensional semiconductors quantum dots (QDs) structures take an important place in fundamental and applied research.[1–4] According to their fabrication process, these quantum dots present different shapes (pyramid,[5–7] sphere,[8,9] lens,[10–12] disk,[13] and arbitrary shape.[14] In quantum dot systems, the additional quantum confinement dramatically changes the optical and electronic properties, compared to those in bulk structures. The confinement effects also influence the excitonic spectrum, which opens other interesting technological possibilities and applications for future quantum information technology and quantum computing.

Zinc oxide (ZnO) is an interesting and versatile material due to its physical properties.[15] With a direct band gap (3.4 eV at 300 K) and a large exciton binding energy (60 meV) providing a strong excitonic emission at room temperature, it is considered as an important material for a wide range of optical applications in various fields: UV detectors, UV light emitters, lasers, window materials for solar cells and piezo devices, optoelectronic devices.[15–19] The PL spectrum of ZnO quantum dots shows two types of emission: a broad green emission band related to deep levels situated in the visible range and the second one located at 3.48 eV in the UV region. Due to their large binding energy, the excitons play an important role in the optical properties of ZnO at room temperature, as demonstrated in the feasibility of polariton lasers[20] and non-linear susceptibility of ZnO nanoparticles: Guo *et al.*[21] have experimentally found that the third order non-linear susceptibility of ZnO nanoparticles is about 500 times larger than that of bulk ZnO.

Generally speaking, because of the important promising properties of ZnO we can retrieve many theoretical and experimental works (for more details see Ref. 15). Gil and Kavokin[22] have shown that the exciton-photon coupling in ZnO QDs is particularly strong and that the exciton radiative recombination rate drastically varies with the dot size. Fonoberov and Balandin[23,24] calculated the radiative lifetime of excitons in ZnO nano-crystals, predicted the size dependence of the exciton radiative lifetime and attempted to explain the origin of the UV luminescence from ZnO QDs, as confirmed later by the experimental and theoretical work by Dalali *et al.*[25] More recently, Dujardin *et al.*[26] discussed the dissociation process of an ionized donor bound exciton (D^+, X) in a ZnO spherical quantum dot (SQD) and estimated the values and the behavior of the Stark shift of the exciton and the (D^+, X) complex.

In the framework of the investigation and exploitation of the properties of this material, we introduce the effect of an external electric field. It is known that under the electric field, the optical transition energy in confined systems is modified leading to a quantum-confined Stark shift (QCSS).[27] Stark shifts effects have been observed in single QDs by photo-luminescence,[28] electro-reflectance,[29] and electroluminescence[30] among other techniques. When the electron and hole are confined in a quantum dot, the application of an external electric field reduces the 1*s* binding energy of the exciton involving a red-shift in the photoluminescence spectrum. This effect is also accompanied by a reduction in the oscillator strength intensity due to the separation of the electron-hole wave function and thus the reduction of the coulombic interaction. The QCSS is characterized by two competing effects: (i) in the strong confinement regime (size below the excitonic Bohr radius) the confinement dominates over electric field, yielding to large emission

a)Electronic address: el-mustapha.feddi@univ-lorraine.fr.

energies and short excitonic lifetime; (ii) in the weak confinement regime (size larger than the excitonic Bohr radius), the Stark effect takes over and we assist to a decrease of the emission energy when the size raises, whereas the exciton lifetime turns up because the oscillator strength reduces.

In relation with this subject, and in order to contribute in the comprehension of the effect of a lateral electric field on excitons in a single ZnO thin disk, we report in this paper a full variational analysis of the QCSS versus confinement in the lateral direction, assuming that the wavefunction is limited to the plane coordinates. We note that the thin disks shaped ZnO synthesized experimentally[31] are characterized by a very large diameter D compared to the height dimension h where $h = 300\,\text{nm}$ and $D = 3\,\mu\text{m}$. We will return to this description in the theoretical part. In Sec. II, we outline the theoretical background of our model. Indeed, our basic theory relies on the effective mass approximation which has been widely used by many authors to describe electronic motion near band gap extrema in the presence of perturbations such as electric fields in low dimensional semiconductors.[32] In the last section, we present our numerical results and we give our conclusion.

II. THEORETICAL FORMALISM

In the framework of the effective mass approximation and considering that the quantum disk and the host material have close dielectric constants (ε) so that the dielectric mismatch can be neglected, the Hamiltonian of an exciton under the effect of an external electric field $\vec{F}$ reads

$$H_X = H_e + H_h - \frac{e^2}{\varepsilon|\vec{r_e} - \vec{r_h}|} + W. \tag{1}$$

$H_i(i = e, h)$ is the unperturbed Hamiltonian of a single particle (electron or hole) in a quantum disk given by

$$H_i = -\frac{\hbar^2}{2m_i^*}\nabla_i^2 + V_i(\rho_i) + V_w^i(z_i). \tag{2}$$

Because the ZnO has a large band gap, we assume that the electron and hole are completely confined in the disk space. In addition, we suppose that the host material has a large band gap, thus the confinement potentials can be well described by a hard wall potential

$$V_i(\rho_i) = \begin{cases} 0 & \rho_i \le R \\ \infty & \rho_i > R \end{cases} \tag{3}$$

and

$$V_w^i(z_i) = \begin{cases} 0 & |z_i| \le h/2 \\ \infty & |z_i| > h/2. \end{cases} \tag{4}$$

The third term in Eq. (1) is the coulombic interaction V_c where ε is the dielectric constant of the semiconductor which takes into account the possible polarization effects. The last term $W = q\vec{F}.(\vec{\rho_e} - \vec{\rho_h})$ is the electrostatic energy due to an applied lateral electric field. In order to study the lateral motion, we consider that for a thin quantum disk ($h \ll R$) submitted to a lateral electric field the exciton behaves like a dipole. The electron and hole orbitals are oriented in opposite sides with respect to the field direction and the system admits strong polarization and polarizability of the charge carriers along the applied field direction. Consequently, the electrostatic interactions can be considered important only in the field direction. Thus, the coulombic potential can be approximated by $-e^2/(\varepsilon\rho_{eh})$ where the in-plane electron-hole distance ρ_{eh} is defined by $\vec{\rho_{eh}} = \vec{\rho_e} - \vec{\rho_h}$. These two approximations permit us to separate the Hamiltonian into two parts: in the z direction which is the well-known problem for a particle in an infinite square well $\left(-\frac{\partial^2}{\partial z^2} + V_w(z)\right)$ and in the plane for the lateral motion. Using the effective excitonic units: $a_X = \varepsilon\hbar^2/e^2\mu$ for length and $R_X = \hbar^2/2\mu a_X$ for energy, where $\mu = m_e^* m_h^*/(m_e^* + m_h^*)$ is the reduced effective mass of the exciton and $e^2 = q^2/(4\pi\varepsilon_0)$, the lateral Hamiltonian expressed in polar coordinates takes the form:

$$H_X = \frac{1}{\sigma+1}H_e + \frac{\sigma}{\sigma+1}H_h - \frac{2}{\rho_{eh}} + f(\rho_e\cos\theta_e - \rho_h\cos\theta_h), \tag{5}$$

where $\sigma = m_e^*/m_h^*$ is the electron-hole mass ratio, $f = F/F_I$ is the reduced electric field, $F_I = R_X/(qa_X)$ corresponds to the 3D ionization field of the exciton and the electric field is supposed oriented in the Ox direction.

For a single particle ($i = e, h$) in the disk and in the absence of electric field, the Hamiltonian operator expressed in polar coordinates and in the effective units of the particle considered reads

$$H_i(\rho_i, \theta_i) = -\left(\frac{\partial^2}{\partial\rho_i^2} + \frac{1}{\rho_i}\frac{\partial}{\partial\rho_i} + \frac{1}{\rho_i^2}\frac{\partial^2}{\partial\theta_i^2}\right) + V_i(\rho_i). \tag{6}$$

The ground state wave function solution of this Hamiltonian operator is $\Psi_i(\rho_i) = J_0\left(\frac{\rho_i}{R}a_0\right)$, where a_0 is the first zero of the cylindrical Bessel function J_0 and the associated energy is given by $(a_0/R)^2$ in the effective units of the particle considered.

In the presence of the coulombic term and the lateral electric field, the problem becomes more complicated and does not admit any analytical solution, so we attempt to determine the excitonic energies levels within a variational method by choosing a trial wave function Ψ_X

$$\Psi_X(\rho_e, \rho_h, \theta_e, \theta_h) = J_0\left(\frac{\rho_e}{R}a_0\right)J_0\left(\frac{\rho_h}{R}a_0\right)\exp(-\eta\rho_{eh}) \times \exp[-\beta f(\rho_e\cos\theta_e - \rho_h\cos\theta_h)], \tag{7}$$

where η and β are two variational parameters and $\rho_{eh} = \sqrt{\rho_e^2 + \rho_h^2 - 2\rho_e\rho_h\cos(\theta_e - \theta_h)}$. The $\exp(-\eta\rho_{eh})$ term describes the coulombic correlations effects between the electron and hole. The last exponential term containing the variational parameter β is chosen by analogy with the trial wave function used in the quantum well case where this choice was tested by several authors leading to good

results.[33–36] So, the exciton ground energy is determined variationally by minimizing the following expression:

$$E_X = \min_{\eta,\beta}\left(\frac{\langle\Psi_X|H_X|\Psi_X\rangle}{\langle\Psi_X|\Psi_X\rangle}\right). \quad (8)$$

First, the H_X operator is applied on Ψ_X and the result depends on the four variables $\rho_e, \rho_h, \theta_e, \theta_h$. However, this coordinates system is not suitable to evaluate the coulombic term $\langle\Psi_X|V_c|\Psi_X\rangle$ which presents a singularity. So, we use a new coordinates system defined on Fig. 1 which avoids this problem and allows to locate unambiguously the two particles. The numerical integrations are performed on $\rho_{eh}, \phi, \rho_h, \theta_h$ in this order with $0 \le \rho_{eh} \le \rho_M$ and $\rho_M = \sqrt{R^2 - \rho_h^2 \sin^2\phi} - \rho_h \cos(\phi)$, $0 \le \phi \le 2\pi$, $0 \le \rho_h \le R$ and $0 \le \theta_h \le 2\pi$.

III. RESULTS AND DISCUSSION

In this work, we apply our model to a ZnO quantum disk of radius R and thickness $h \ll R$. Before to discuss our results, we recall that for ZnO materials there are many controversies in literature about the real value of the heavy hole mass m^*_{hh} ranging from $0.59m_0$ to $2.27m_0$. Indeed, the experimental reports on the effective hole mass are relatively very few, most probably limited by the measurement techniques employed and the quality of the materials used. Recent theoretical calculations[37] have shown that m^*_{hh} is more than 2. On the other hand, several authors consider that for the heavy hole mass two values are available: $m^*_{hh} = 0.59m_0$ from calculation of the free exciton binding energy and $m^*_{hh} = 0.78m_0$ from calculation of the excitonic transition in ZnO/ZnMgO heterostructures.[38,39] More recently, we have shown[26] that the theoretical calculation of the exciton energy in a ZnO SQD fits quite well with the experimental data using $m^*_{hh} = 0.78m_0$. On the other hand, we outline that the choice of the value of the dielectric constant will considerably modify the coulombic potential and consequently the exciton binding energy. Indeed, the problem in the determination of effective masses from the optical spectra is the value of the dielectric constant used in computation. In a recent study, Yang *et al.*[19] show that the experimental values of the dielectric constant fit linearly with the dot radius in a single ZnO nanowire and range from 6.2 to 6.8. In the present study and in order to retrieve the bulk ZnO binding energy (~60 meV), we adopt the same physical parameters than Morhain *et al.*:[40] $m^*_e = 0.24m_0$, $m^*_{hh} = 0.78m_0$, and the dielectric constant $\varepsilon = 6.4$. Thus, the values of excitonic Bohr radius, excitonic Rydberg energy, and electric field ionization are $a_X = 1.85$ nm, $R_X = 60.96$ meV, and $F_I = 330$ kV/cm.

In order to study the correlation of the electron and hole in a lateral electric field, we present in Fig. 2 the evolution of the excitonic binding energy as a function of radius for some values of electric field strength $F = 0$, 200, 400, and 600 kV/cm. We use the classic definition for the excitonic binding energy given by the difference between the non-correlated and correlated electron-hole pair ($E_b = E_e + E_h - E_X$) where the energy of the uncorrelated pair $E_e + E_h$ is obtained by omitting the coulombic term $-\frac{2}{\rho_{eh}}$ in Eq. (5) and setting $\eta = 0$ in Eq. (7). We can see that the electric field shifts down the excitonic binding energies. Indeed, with a lateral applied electric field, there exists a competition between three conflicting effects: the confinement effect ($\sim 1/R^2$), the attractive coulombic effect ($\sim -1/R$), and the negative dipolar effect which depends on the electric field strength. The confinement effect tends to reduce the spatial extension of the excitonic wave function while the electric field tends to move the electron and hole densities in opposite directions which implies a decrease of the overlap of the electron and the hole wave

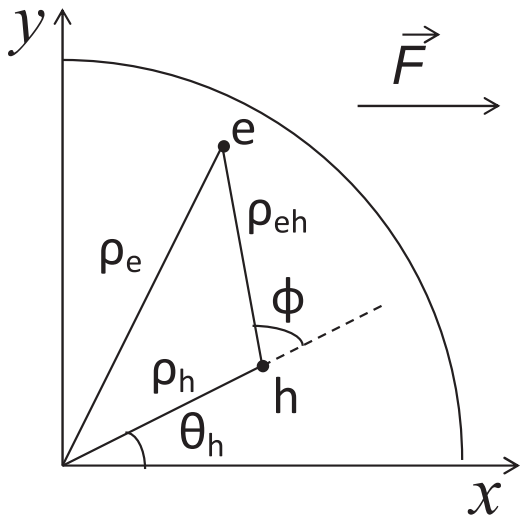

FIG. 1. Diagram of system coordinates.

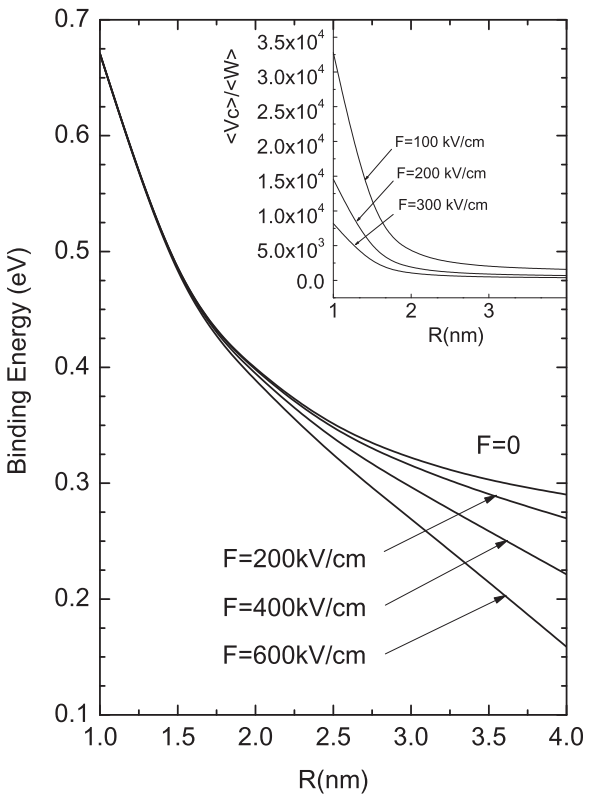

FIG. 2. Exciton binding energy vs the disk radius for several values of electric field strength: $F = 0$, 200, 400, and 600 kV/cm. The inset shows the ratio $\frac{\langle V_c\rangle}{\langle W\rangle}$ as a function of the disk radius for $F = 100$, 200, and 300 kV/cm.

functions. For R less than a_X, the strong confinement is predominant and the exciton wave function is more localized so the charge distribution is less sensitive to the electric field. Thus, the curves corresponding to different values of F coincide and the energy decreases with increasing R. In the case of $R > a_X$, the influence of the electric field is more pronounced due to the fact that excitonic orbital is more extended: by increasing the dot size, the confinement effect becomes negligible and only the coulombic attraction competes with the dipolar electric energy so we assist to a splitting of all curves.

As we can see in the inset of Fig. 2, we plot the variation of the ratio $\frac{\langle V_c \rangle}{\langle W \rangle}$ as a function of dot size for three electric field strengths ($F = 100$, 200, 300 kV/cm). We remark that in all cases the effect of the coulombic potential is usually predominant and tends to zero for large R which proves that the exciton exists and does not collapse for these values of electric field strength. In addition, the ratio $\frac{\langle V_c \rangle}{\langle W \rangle}$ decreases with increasing disk radius for a given F because the coulombic potential decreases when R increases and the large space in the disk makes easier the electron-hole separation by the electric field. But in the strong confinement regime, the attractive nature of the coulombic potential is very important due to the confinement effect. We note that at zero field ($F = 0$) the nanodisk band gap $E_g^{QD} = E_g^{bulk} + E_e + E_h - E_b$ has a non significative variation for large disk size thus the blue shift is expected to occur for the strong confinement. The same conclusion was established by Tan *et al.*[41] using PL emission in thin films of ZnO. They have shown that E_g^{QD} variation is negligible for R ranging between 2.4 and 6 nm and the PL emission does not present a blue shift due to the weak confinement.

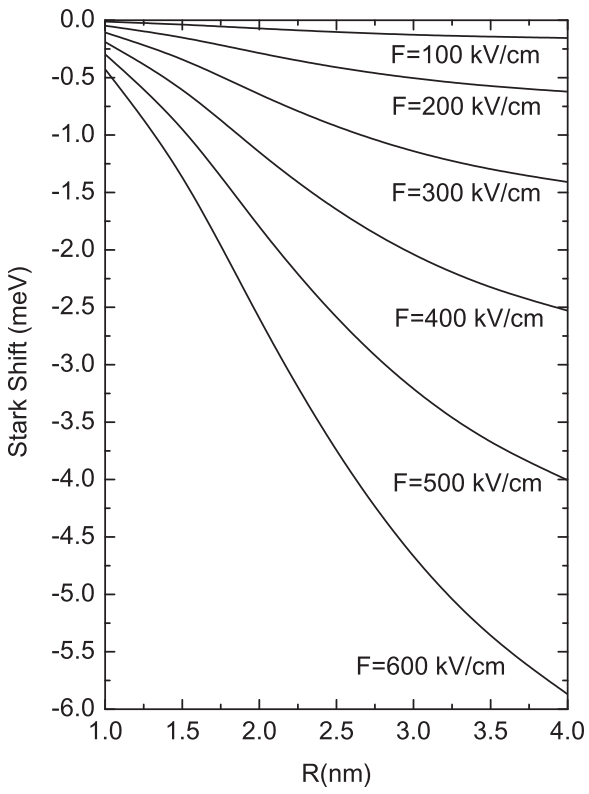

FIG. 3. Variations of the exciton lateral Stark shift as a function of the disk radius for different values of the electric field strength.

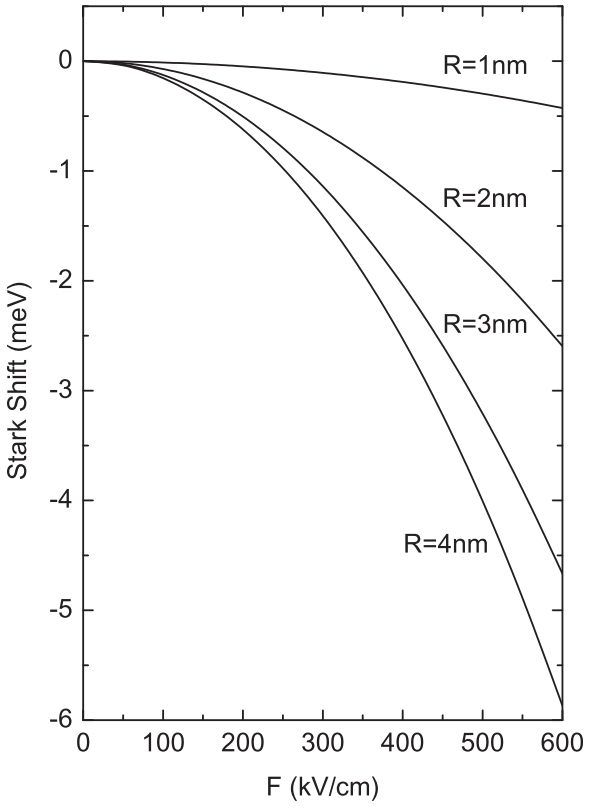

FIG. 4. The exciton Stark shift vs the electric field strength for different confinement regimes $R = 1$, 2, 3, and 4 nm.

In the aim to understand the effect of the electric field, we analyze the Stark shift as a function of the disk radius and the electric field strength. By setting $f = 0$ in Eqs. (5) and (7), we obtain the excitonic energy without electric field and we define the Stark shift by $\Delta E = E(F) - E(0)$, where $E(F)$ and $E(0)$ are the exciton energies with and without electric field, respectively. In Fig. 3, we plot the exciton Stark shift versus the disk size for electric field strength from 100 kV/cm to 600 kV/cm. This figure shows that the Stark shift decreases as the radius increases for a given electric field and the decrease is more pronounced for higher field strengths. For large sizes, the Stark shift is more important but tends to a saturation which means that the exciton remains stable and does not collapse even for large applied electric field equal to $2F_I$.

In Fig. 4, we plot the Stark shift as a function of the electric field for different disk radii from 1 nm to 4 nm. We remark that for a strong confinement ($R = 1$ nm), the Stark shift is not significative with increasing electric field. For $R > a_X$, the Stark shift becomes obvious and more important with increasing electric field because the lateral applied electric field leads to an easier separation of electron and hole

TABLE I. Induced dipole moment p and polarizability α.

R(nm)	1	2	3	4
$p(\mu\text{eV cm kV}^{-1})$	5.6×10^{-2}	21.42	151.60	330.37
$\alpha(\mu\text{eV cm}^2\text{ kV}^{-2})$	1.19	7.24	13.17	16.76

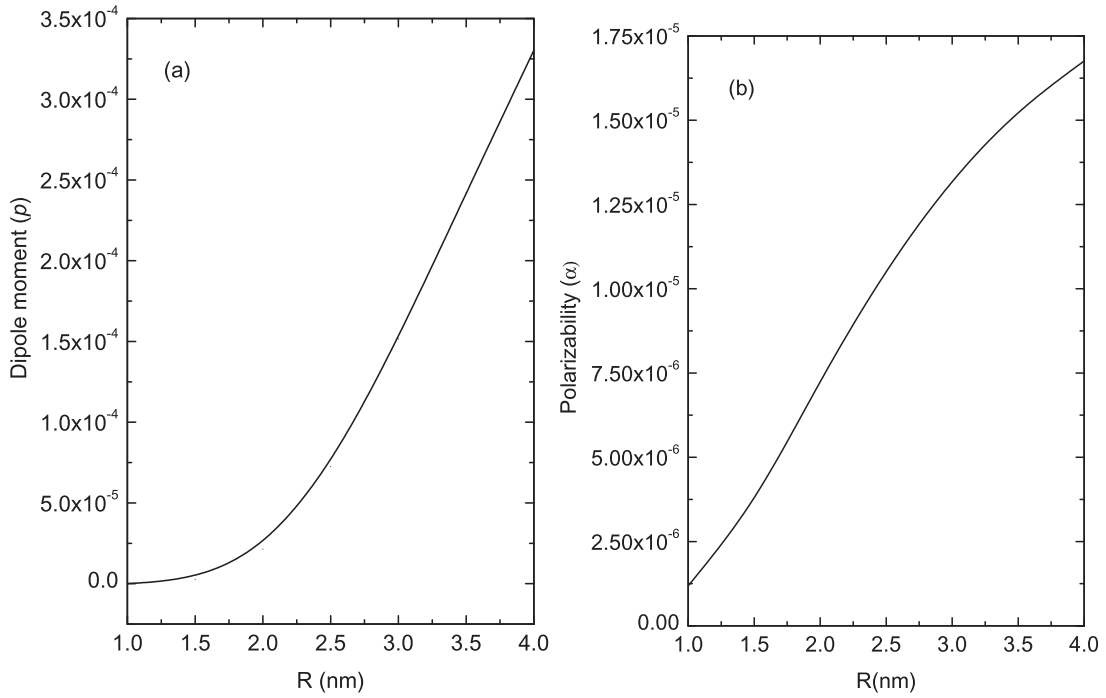

FIG. 5. Fit results of: (a) the exciton lateral induced dipole moment p ($\mathrm{eV\,cm\,kV^{-1}}$), (b) the exciton lateral polarizability α ($\mathrm{eV\,cm^2\,kV^{-2}}$), as functions of the disk radius R.

orbitals, which reduces the overlap of their wave functions. The negative curvature of the Stark shift depends strongly on the disk size. For weak confinement, the energy shift tends to be linear with increasing electric field.

In order to clarify this point of view, let us consider the analogy with the theory of perturbation in the hydrogen atom: the Stark shift can be written as $\Delta E = E(F) - E(0) \simeq pF - \alpha F^2$, where p and α are, respectively, the induced dipole moment and the polarizability in the direction of the applied electric field. In the quantum confined system, the spatial separation of the charge carriers under the lateral electric effect diminishes the e-h interaction and leads to a blue shift which compensates the red shift caused by the electric field. The existence of the polarization p and the sign of α were the subject of some discussions in the literature (for more details we refer the reader to Refs. 42 and 43). The result of the fit of all curves given in Fig. 4 using the perturbative form of the Stark shift mentioned above is given in Table I for the three types of confinement.

Our results show that the polarizability α is always positive corresponding to a red shift and increases with increasing disk size. The fit reveals that in all cases, the Stark shift possesses nonzero linear and quadratic contributions, indicating that the component of the induced dipole in the lateral direction is significant especially for $R \gtrsim a_X$ which is experimentally proved in the InGaN quantum disk.[44,45] In strongly confined QDs, the electric field induces a large polarizability. The positive sign of p indicates that this term compensates the red shift. Figs. 5(a) and 5(b) show the resulting predictions for the variations of p and α as functions of the disk size. Some information can be extracted from these figures. Concerning the induced dipole moment, it is very sensitive to the dot radius and in the case of ZnO it takes an important value for large size dots ($330\,\mu\mathrm{eV\,cm\,kV^{-1}}$ for $R = 4$ nm). Our calculations show that p admits a positive value for all dot sizes which implies that the first order Stark shift has a positive contribution in the excitonic energy resulting in PL by a blue shift. On the other hand, the polarizability preserves always positive values indicating that the quadratic Stark shift is negative leading to a red shift. We want to underline that these results prove the existence of a correlation between the polarizability and the dipole moment which influences the ZnO quantum disk optical properties.

IV. CONCLUSION

In conclusion, we have used the lateral electric field to explore its effect on excitons confined in a ZnO thin quantum disk. Our approach shows the existence of two contributions when applying an electric field: linear (induced dipole) and quadratic (QCSS) terms. Both terms are strongly correlated and are very sensitive to the quantum disk size. These calculations can be easily translated to recently proposed semiconductors chemically synthesized in the form of nanoflakes (CdS, CdSe, CdTe, PbS, GaSe).[46–48] This behavior can be used as a tool to adjust and tailor the nanodisk for new optoelectronic applications, such as emitters, electro-optical modulators, and photodetectors. Such effects open the possibility to realize logic gates controlled by an external electric field for the development of quantum computing as well as optical memories and switches.[49]

ACKNOWLEDGMENTS

This work was supported by the Hassan II Academy of Science and Technology (Morocco), the Generalitat

Valenciana Grant PROMETEO/2009/074, and the Spanish MINECO Project TEC2011-29120-C05-01.

[1]A. D. Yoffe, Adv. Phys. **42**, 173 (1993).
[2]A. D. Yoffe, Adv. Phys. **50**, 1 (2001).
[3]L. Banyai and S. W. Koch, *Semiconductor Quantum Dots* (World Scientific, Singapore, 1993).
[4]P. Hawrylak and M. Korkusinski, *Single Quantum Dots: Fundamentals, Applications, and New Concepts*, Topics in Applied Physics Vol. 90, edited by P. Michler (Springer-Verlag, Berlin).
[5]M. A. Cusack, P. R. Briddon, and M. Jaros, Phys. Rev. B **54**, R2300 (1996).
[6]C. Pryor, Phys. Rev. B **57**, 7190 (1998).
[7]M. Grundmann, O. Stier, and D. Bimberg, Phys. Rev. B **52**, 11969 (1995).
[8]J. L. Marín, R. Riera, and S. A. Cruz, J. Phys.: Condens. Matter **10**, 1349 (1998).
[9]T. Uozumi, Y. Kayanuma, K. Yamanaka, K. Edamatsu, and T. Itoh, Phys. Rev. B. **59**, 9826 (1999).
[10]C. Cornet, J. Even, and S. Loualiche, Phys. Lett. A **344**, 457 (2005).
[11]A. Forchel, R. Steffen, T. Koch, M. Michel, M. Albrecht, and T. L. Reinecke, Semicond. Sci. Technol. **11**, 1529 (1996).
[12]E. Assaid, M. Aydi, E. Feddi, and F. Dujardin, Cent. Eur. J. Phys. **6**(1), 97 (2008).
[13]E. Menéndez-Proupin, C. Trallero-Giner, and S. E. Ulloa, Phys. Rev. B **60**, 16747 (1999).
[14]A. A. Kiselev, K. W. Kim, and M. A. Stroscio, Phys. Rev. B **60**, 7748 (1999).
[15]Ü. Özgür, Ya. I. Alivov, C. Liu, A. Teke, M. A. Reshchikov, S. Doğan, V. Avrutin, S.-J. Cho, and H. Morkoç, J. Appl. Phys. **98**, 041301 (2005).
[16]M. H. Huang, S. Mao, H. Feick, H. Yan, Y. Wu, H. Kind, E. Weber, R. Russo, and P. Yang, Science **292**, 1897 (2001).
[17]K. Keis, E. Magnusson, H. Lindstrom, S. E. Lindquist, and A. Hagfeldt, Sol. Energy Mater. Sol. Cells **73**, 51 (2002).
[18]D. Gruber, F. Kraus, and J. Muller, Sens. Actuators B **92**, 81 (2003).
[19]Y. Yang, W. Guo, X. Wang, Z. Wang, J. Qie, and Y. Zhang, Nano Lett. **12**, 1919 (2012).
[20]D. Vanmaekelbergh and L. K. van Vugt, Nanoscale **3**, 2783 (2011).
[21]L. Guo, S. Yang, C. Yang, P. Yu, J. Wang, W. Ge, and G. K. L. Wong, Appl. Phys. Lett. **76**, 2901 (2000).
[22]B. Gil and A. V. Kavokin, Appl. Phys. Lett. **81**, 748 (2002).
[23]V. A. Fonoberov and A. A. Balandin, Appl. Phys. Lett. **85**, 5971 (2004).
[24]V. A. Fonoberov and A. A. Balandin, Phys. Rev. B **70**, 195410 (2004).
[25]L. Dallali, S. Jaziri, J. Haskouri, P. El Haskouri, P. Ramos, and J. Martinez-Pasor, Solid State Commun. **151**, 822 (2011).
[26]F. Dujardin, E. Feddi, E. Assaid, and A. Oukerroum, Eur. Phys. J. B **74**, 507 (2010).
[27]D. A. B. Miller, D. S. Chemla, T. C. Damen, A. C. Gossard, W. Wiegmann, T. H. Wood, and C. A. Burrus, Phys. Rev. B **32**, 1043 (1985).
[28]S. Sanguinetti, M. Gurioli, E. Grilli, M. Guzzi, and M. Henini, Appl. Phys. Lett. **77**, 1982 (2000).
[29]P. Jin, C. M. Li, Z. Y. Zhang, F. Q. Liu, Y. H. Chen, X. L. Ye, B. Xu, and Z. G. Wang, Appl. Phys. Lett. **85**, 2791 (2004).
[30]I. E. Itskevich, S. I. Rybchenko, I. I. Tartakovskii, S. T. Stoddart, A. Levin, P. C. Main, L. Eaves, M. Henini, and S. Parnell, Appl. Phys. Lett. **76**, 3932 (2000).
[31]C. X. Xu, X. W. Sun, Z. L. Dong, and M. B. Yu, Appl. Phys. Lett. **85**, 3878 (2004).
[32]M. G. Burt, J. Phys.: Condens. Matter **4**, 6651 (1992).
[33]H. Ham and H. N. Spector, Physica B **381**, 53–56 (2006).
[34]G. J. Vasquez, M. del Castillo-Mussot, and H. N. Spector, Phys. Status Solidi B **240**, 561 (2003).
[35]G. Bastard, E. E. Mendez, L. L. Chang, and L. Esaki, Phys. Rev. B **28**, 3241 (1983).
[36]F. Dujardin, A. Oukerroum, E. Feddi, J. Bosch Bailach, J. Martínez-Pastor, and M. Zazi, J. Appl. Phys. **111**, 034317 (2012).
[37]W. R. L. Lambrecht, A. V. Rodina, S. Limpijumnong, B. Segall, and B. K. Meyer, Phys. Rev. B **65**, 075207 (2002).
[38]B. K. Meyer, J. Sann, S. Lautenschläger, M. R. Wagner, and A. Hoffmann, Phys. Rev. B **76**, 184120 (2007).
[39]G. Coli and K. K. Bajaj, Appl. Phys. Lett. **78**, 2861 (2001).
[40]C. Morhain, T. Bretagnon, P. Lefebvre, X. Tang, P. Valvin, T. Guillet, B. Gil, T. Taliercio, M. Teisseire-Doninelli, B. Vinter, and C. Deparis, Phys. Rev. B **72**, 241305R (2005).
[41]S. T. Tan, B. J. Chen, X. W. Sun, W. J. Fan, H. S. Kowk, X. H. Zhang, and S. J. Chua, J. Appl. Phys. **98**, 013505 (2005).
[42]S. Ritter, P. Gartner, N. Baer, and F. Jahnke, Phys. Rev. B **76**, 165302 (2007).
[43]M. Korkusinski, M. E. Reimer, R. L. Williams, and P. Hawrylak, Phys. Rev. B **79**, 035309 (2009).
[44]J. Robinson, J. Rice, K. Lee, J. Na, R. Taylor, D. Hasko, R. Olivier, M. Kappers, C. Humpherys, and G. Briggs, Appl. Phys. Lett. **86**, 213103 (2005).
[45]R. J. Warburton, C. Schulhauser, D. Haft, C. Schäflein, K. Karrai, J. M. Garcia, W. Schoenfeld, and P. M. Petroff, Phys. Rev. B **65**, 113303 (2002).
[46]S. Ithurria, M. D. Tessier, B. Mahler, R. P. S. M. Lobo, B. Dubertret, and Al. L. Efros, Nature Mater. **10**, 936 (2011).
[47]C. Schliehe, B. H. Juarez, M. Pelletier, S. Jander, D. Greshnykh, M. Nagel, A. Meyer, S. Foerster, A. Kornowski, C. Klinke, and H. Weller, Science **329**, 550 (2010).
[48]P. Hu, Z. Wen, L. Wang, P. Tan, and K. Xiao, ACS Nano **6**, 5988 (2012).
[49]V. Stavarache, D. Reuter, A. D. Wieck, M. Schwab, D. R. Yakovlev, R. Oulton, and M. Bayer, Appl. Phys. Lett. **89**, 123105 (2006).